ACADEMIC
PRESS

Wavelets on the sphere: implementation and approximations

J.-P. Antoine,[a,*] L. Demanet,[a,1] L. Jacques,[a] and P. Vandergheynst[b]

[a] *Institut de Physique Théorique, Université Catholique de Louvain, B 1348, Louvain-la-Neuve, Belgium*
[b] *Signal Processing Laboratory, Swiss Federal Institute of Technology (EPFL), CH 1015, Lausanne, Switzerland*

Abstract

We continue the analysis of the continuous wavelet transform on the 2-sphere, introduced in a previous paper. After a brief review of the transform, we define and discuss the notion of directional spherical wavelet, i.e., wavelets on the sphere that are sensitive to directions. Then we present a calculation method for data given on a regular spherical grid $\mathcal{G}$. This technique, which uses the FFT, is based on the invariance of $\mathcal{G}$ under discrete rotations around the z axis preserving the φ sampling. Next, a numerical criterion is given for controlling the scale interval where the spherical wavelet transform makes sense, and examples are given, both academic and realistic. In a second part, we establish conditions under which the reconstruction formula holds in strong L^p sense, for $1 \leqslant p < \infty$. This opens the door to techniques for approximating functions on the sphere, by use of an approximate identity, obtained by a suitable dilation of the mother wavelet.
© 2002 Elsevier Science (USA). All rights reserved.

Keywords: Continuous wavelet transform; 2-sphere; Directional spherical wavelet; Approximate identity

1. Introduction: the spherical continuous wavelet transform

In a previous paper [6], two of us have introduced a continuous wavelet transform (CWT) on the 2-sphere S^2, using the general construction of coherent states on manifolds developed in [1,2]. We will pursue this study here and focus on three aspects left out in [6], namely the extension to anisotropic wavelets, the practical implementation of the transform with a (reasonably) fast algorithm and its application to the problem of approximation of functions on S^2 (in L^p sense).

The key point of the spherical CWT is that it lives entirely on the sphere (signals and wavelets) and it is derived from invariance considerations, via group-theoretical methods. First, one identifies the affine transformations of S^2: Motions, which are realized by rotations $\varrho \in SO(3)$, and local dilations, which are obtained by lifting to S^2, by inverse stereographical projection, the usual dilations in the plane tangent at the North Pole. Then one shows that these transformations may be embedded (via the Iwasawa decomposition) into the conformal group of S^2, which is the Lorentz group $SO_0(3, 1)$. The latter possesses

---

a natural unitary irreducible representation in the space $L^2(S^2)$ of finite energy signals on S^2, and this representation is square integrable over the parameter space $SO(3) \times \mathbb{R}_*^+$ of the CWT (see [6] for the precise mathematical definitions). As a consequence, a genuine CWT may be set up according to the general scheme of [1,2].

In order to fix our notations and make the paper reasonably self-contained, we recall first the essential facts, referring to [6] for the details. The spherical coordinates on S^2 are denoted by $\omega = (\theta, \varphi)$ and the space of finite energy signals by $L^2(S^2) \equiv L^2(S^2, \mathrm{d}\mu)$, where $\mathrm{d}\mu(\omega) = \sin\theta \, \mathrm{d}\theta \, \mathrm{d}\varphi$ is the usual (rotation invariant) measure on S^2. The affine transformations on S^2 are realized in $L^2(S^2)$ by the following unitary operators:

- Motions:

$$(R_\varrho f)(\omega) = f(\varrho^{-1}\omega) = (U_{\mathrm{qr}}(\varrho)f)(\omega), \quad \varrho \in SO(3), \tag{1.1}$$

  where U_{qr} is the (infinite-dimensional) quasi-regular representation of $SO(3)$ in $L^2(S^2)$.

- Dilations:

$$(D_a f)(\omega) \equiv f_a(\omega) = \lambda(a,\theta)^{1/2} f(\omega_{1/a}), \quad a \in \mathbb{R}_*^+, \tag{1.2}$$

  where $\omega_a \equiv (\theta_a, \varphi)$ and $\tan(\theta_a/2) = a\tan(\theta/2)$ (indeed, $\theta \mapsto \theta_a$ is the dilation obtained by inverse stereographical projection). Here $\lambda(a,\theta)$ is the cocycle (Radon–Nikodym derivative) which expresses the noninvariance of the measure μ under dilation, and it is given by

$$\lambda(a,\theta) = \frac{4a^2}{[(a^2 - 1)\cos\theta + (a^2 + 1)]^2}.$$

A *spherical wavelet* is a function $\psi \in L^2(S^2)$ that is an admissible vector for the representation of the Lorentz group mentioned above. The admissibility condition reads as

$$G_l \equiv \frac{8\pi^2}{2l+1} \sum_{|m| \leqslant l} \int_0^\infty \frac{\mathrm{d}a}{a^3} |\widehat{\psi}_a(l,m)|^2 < c, \tag{1.3}$$

where $\hat{f}(l,m) \equiv \langle Y_l^m | f \rangle$ denotes a Fourier coefficient of $f \in L^2(S^2)$ and the constant $c > 0$ is independent of l. This condition is not easy to use. However, a necessary (and almost sufficient) condition for admissibility is the zero mean condition

$$C_\psi \equiv \int_{S^2} \mathrm{d}\mu(\theta, \varphi) \frac{\psi(\theta, \varphi)}{1 + \cos\theta} = 0. \tag{1.4}$$

Typical admissible wavelets are the difference wavelets

$$\psi_\phi^{(\alpha)}(\theta, \varphi) = \phi(\theta, \varphi) - \frac{1}{\alpha} D_\alpha \phi(\theta, \varphi), \quad \alpha > 1, \tag{1.5}$$

for a given smoothing function $\phi \in L^2(S^2)$. The most familiar one is the spherical DOG wavelet $\psi_G^{(\alpha)}$, corresponding to a Gaussian smoothing function $\phi_G(\theta, \phi) = \exp(-\tan^2(\theta/2))$, $\theta \in [-\pi, \pi]$, i.e., a Gaussian centered on the North Pole of the sphere.

Then, given an admissible wavelet ψ, the family $\{\psi_{a,\varrho} \equiv R_\varrho D_a \psi = R_\varrho \psi_a, \varrho \in SO(3), a > 0\}$ is an overcomplete set of functions in $L^2(S^2)$ and even a continuous frame, nontight in general.

Accordingly, the spherical CWT of a signal $s \in L^2(S^2)$ is defined as

$$S(\varrho, a) = \langle \psi_{a,\varrho} | s \rangle = \int_{S^2} \mathrm{d}\mu(\omega) \overline{[R_\varrho D_a \psi](\omega)} s(\omega)$$

$$= \int_{S^2} \mathrm{d}\mu(\omega) \overline{\psi_a(\varrho^{-1}\omega)} s(\omega). \tag{1.6}$$

It is instructive to split $\varrho \in SO(3)$ into $\varrho = (\chi, [\omega'])$ with $\chi \in SO(2)$ and $\omega' \in S^2$. This is formally done through a projection $\varrho \mapsto \omega'(\varrho)$ in the fiber bundle $S^2 \simeq SO(3)/SO(2)$ followed by an arbitrary choice of section $\omega' \mapsto [\omega']$ in $SO(3)$. The splitting corresponds to decomposing the motion R_ϱ of the wavelet ψ_a into an initial rotation of angle χ around the North Pole ω_0 followed by a transport to the point $\omega' = \varrho \omega_o$ on the sphere (these two operations could have been defined in the reverse order). In other words,

$$R_\varrho \psi_a(\omega) = R_\chi \psi_a([\omega']^{-1}\omega),$$

where R_χ is a rotation around the North Pole. Accordingly, the spherical wavelet transform will also be denoted by $S(\chi, \omega', a)$. Of course, the dependence on χ can be dropped if the wavelet ψ is axisymmetric. We will have a closer look at the consequences of anisotropy for the spherical wavelet transform in Section 2.

The admissibility of the wavelet ψ is sufficient to guarantee the invertibility of the transform, i.e., one may reconstruct the signal s from its transform S. More precisely,

$$s(\omega) = \int\limits_{\mathbb{R}_*^+} \int\limits_{SO(3)} \frac{da \, d\varrho}{a^3} S(\varrho, a) A^{-1} \psi_{a,\varrho}(\omega), \tag{1.7}$$

where $d\varrho$ is the invariant Haar measure on the group $SO(3)$ and A is the frame operator, whose action is a multiplication in the Fourier space,

$$\widehat{Af}(l, m) = G_l \hat{f}(l, m)$$

with G_l defined in the admissibility condition (1.3). As usual, the integral in (1.7) is to be taken in the weak sense. Again, if the wavelet ψ is axisymmetric, the transform reads $S(\omega', a)$ and the integral over $SO(3)$ is replaced by an integral over S^2, with respect to the measure $d\mu$

$$s(\omega) = \int\limits_{\mathbb{R}_*^+} \int\limits_{S^2} \frac{da \, d\mu(\omega')}{a^3} S(\omega', a) \, A^{-1} \psi_{a,\omega'}(\omega). \tag{1.8}$$

At this point, three questions arise. First, what are the concepts involved and what can we expect from the additional rotation parameter χ when the wavelet is not axisymmetric? After discussing the definition, we present in Section 2 a constructive procedure for designing directional wavelets on the sphere. Doing so, we extend the directional analysis capabilities of the CWT to the sphere. This could be important for applications, since many directional features (roads, streams, geological faults, . . .) abound on the spherical Earth!

Second, does this spherical CWT yield a practical analysis tool for signals on the sphere, as its flat space counterpart? In particular, can one design a (reasonably) fast algorithm for a transform that is more general than a convolution on the sphere? Indeed one cannot rely on what has been done with the fast spherical harmonic transform [13,16,17], because of the rotation parameter χ. Preliminary results were given in [6], and we confirm them here. We present in Section 3 an efficient algorithm, following an approach similar to that of Windheuser [25], that is, using an FFT over the longitude angle φ. Several examples are given.

Third, the reconstruction formula (1.7) is valid only in the weak sense. In the flat case, however, the corresponding formula holds in the strong L^2 sense [7,23]. This guarantees that it can be used for approximating functions on the plane through an approximate identity. That means, convolution with a smoothing kernel, which tends to the identity (δ function) as the parameter goes to 0. We show in Section 4 that exactly the same situation prevails on the sphere [24]. First one switches to an L^1 formalism (as already mentioned in [6]), introducing a modified dilation operator D^a that preserves the L^1 norm of functions. It turns out that the operator D^a generates an approximate identity in $L^p(S^2)$ for every $p \in [1, \infty]$, and this shows that the reconstruction formula (1.7) actually holds in strong L^p sense. In this way, we recover the approximation scheme developed by Freeden et al. and applied by them extensively to geophysical data [10,11]. These authors consider various approximation kernels and introduce a form of discrete wavelet transform, through a kind of multiresolution on S^2. By contrast, our approach has the advantage of giving to the approximation parameter the clear meaning of a local dilation factor, thus grounding

the approximation scheme in the general continuous wavelet theory, itself based on group-theoretical considerations.

2. A closer look at the anisotropic spherical CWT

In this section, we aim at giving a clear meaning to the rotation parameter χ, which was not considered in [6]. We discuss the notion of direction on the sphere and how this is related to the ability of performing a directional analysis of data defined on a sphere by means of the spherical wavelet transform. We also build examples of anisotropic spherical wavelets in Section 2.2.

2.1. Remarks on the definition

Whenever the wavelet ψ is not axisymmetric, the continuous spherical wavelet transform depends on the additional parameter χ. This is written as

$$S(\chi, \omega', a) = \int\limits_{S^2} d\mu(\omega) \, \overline{R_\chi \psi_a([\omega']^{-1}\omega)} s(\omega).$$

In this formula, there is an arbitrariness in the way the rotation $[\omega']$ of $SO(3)$ is associated to the point ω' on the sphere. The map $[\cdot]: S^2 \to SO(3)$, called a *section* in group theory, can be depicted as mapping the sphere to a tangent vector field of unit length defined on it. Indeed, there are infinitely many ways of choosing the direction of each tangent vector in the tangent plane. From a practical viewpoint, however, some choices are better than other ones for a given section. It should preferably be smooth to correspond to the idea of *direction* defined on the sphere. Therefore, we expect the values of the wavelet transform to correspond to filtering in a given direction χ and at a given scale a like in the case of the two-dimensional wavelet transform in the plane [4].

Some caution should be exercised, however, when dealing with directions on the sphere. It is a classical result in topology that there exists no differentiable vector field of constant norm on S^2, which means there is no *global* way of defining directions. There will always be some singular point where the definition fails.[2] In other words, one cannot comb a perfectly spherical porcupine! Therefore, testing orientations on the sphere using directional wavelets is necessarily a small scale operation, that is, a *local* procedure. This ability to perform local analysis is definitely one of the most important properties of wavelet analysis.

From now on, we will make use of the classical parametrization of $SO(3)$ in terms of Euler angles, $\varrho \equiv (\chi, \theta', \varphi')$, which corresponds to the choice of section $(\theta', \varphi') \mapsto (0, \theta', \varphi')$, which in turn defines a direction on the sphere. The singular points are the North and South Poles: it makes no sense to define cardinal points at the poles!

For this choice of parametrization, we may write

$$R_\chi \psi_a([\omega']^{-1}\omega) = \psi_{a,\chi,\omega'}(\omega) \equiv \psi_{a,\chi,\theta',\varphi'}(\theta, \varphi), \tag{2.1}$$

which implies

$$\psi_{a,\chi,\theta',\varphi'}(\theta, \varphi) = \psi_{a,\chi,\theta',0}(\theta, \varphi - \varphi'). \tag{2.2}$$

Therefore, (1.6) becomes a convolution in φ which, by means of the convolution theorem, takes the form

$$S(\chi, \theta', \varphi', a) = \int\limits_0^\pi \int\limits_0^{2\pi} \overline{\psi_{a,\chi,\theta',0}(\theta, \varphi - \varphi')} s(\theta, \varphi) \sin\theta \, d\theta \, d\varphi \tag{2.3}$$

$$= 2\pi \sum\limits_{k=-\infty}^{\infty} e^{ik\varphi'} \int\limits_0^\pi \overline{\check{\psi}_{\chi,\theta',0,a}(\theta)[k]} \check{s}(\theta)[k] \sin\theta \, d\theta, \tag{2.4}$$

---

[2] This is valid for S^2, but not in the case of the circle S^1 and the higher dimensional spheres S^3 and S^7.

where, for any function $h : S^2 \to \mathbb{R}$,

$$\check{h}(\theta)[k] = \int\limits_0^{2\pi} d\varphi \, h(\theta, \varphi) \, e^{-i k \varphi} \qquad (2.5)$$

is the Fourier series of h in the longitudinal coordinate φ.

In the discretization step of Section 3, the relations (2.3)–(2.4) will give us a tool for reducing the computational time of the spherical CWT. Indeed, they will allow us to use the fast Fourier transform (FFT), like in [25].

2.2. Directional wavelets

We have not yet addressed the problem of constructing good directional wavelets on S^2. In this section, we will quickly show that this job is naturally handled in our framework. First of all, we recall that the very definition of a direction on S^2 forces us to work at small scales. As we are all familiar with, the geometry of S^2 at small scales, or for large radii of the sphere, is closer and closer to that of $\mathbb{R}^2$. As proved in [5], the spherical wavelet transform respects one's intuition by closely approximating the Euclidean wavelet transform at small scales. This is a property known as the Euclidean Limit, and we may remark that he notation used in (2.1) is consistent with it: Roughly speaking, as the radius of the sphere goes to infinity, $\psi_{a,\chi,\omega'}(\omega)$ goes to $\psi_{a,\chi,\boldsymbol{b}}(\boldsymbol{x})$, where $\boldsymbol{b} \in \mathbb{R}^2$ is the translation parameter [6].

Moreover, it is a simple application of the Euclidean Limit to show that small scale Euclidean wavelets can be mapped to the sphere and yield small scale admissible *spherical* wavelets. These can then be dilated at larger scales using the spherical dilation. This is neatly summarized by the following result [6].

Proposition 2.1. *Let $\psi \in L^2(\mathbb{R}^2)$ be an admissible two-dimensional Euclidean wavelet. The inverse stereographic projection of a square integrable function is defined, in polar coordinates, by*

$$\left(\Pi^{-1} f\right)(\theta, \varphi) = \frac{2 f(2 \tan(\theta/2), \varphi)}{1 + \cos \theta},$$

and is in $L^2(S^2)$. Then the function $\Pi^{-1} \psi$ is an admissible spherical wavelet for the transform defined with the dilation preserving the L^2 norm. The function $\Pi^{-1} \psi / (1 + \cos \theta)$ is an admissible spherical wavelet for the transform defined with the dilation preserving the L^1 norm.

This result tells us that we can construct a spherical wavelet starting from any Euclidean wavelet. Now what does this tell us about directional wavelets? Since directional sensitivity is a local or small scale attribute, it should intuitively survive this process. But there is more than intuition in this result. The stereographic projection and both spherical and Euclidean dilations are conformal mappings. Thus Proposition 2.1 defines a conformal application that, by definition, preserves angles. The directional sensitivity of the Euclidean wavelet is thus transported to the spherical wavelet.

A natural candidate for building a directional spherical wavelet is to start with the Euclidean Morlet or Gabor wavelet [3]

$$\psi_M(\vec{x}) = e^{i \vec{k}_0 \cdot \vec{x}} e^{-\|\vec{x}\|^2}. \qquad (2.6)$$

Using Proposition 2.1, we find the following spherical wavelet:

$$\psi_M(\theta, \varphi) = \frac{e^{i k_0 \tan(\theta/2) \cos(\varphi_0 - \varphi)} e^{-(1/2) \tan^2(\theta/2)}}{1 + \cos \theta}. \qquad (2.7)$$

This function is represented in Figs. 1 and 2 for various values of the scale and rotation parameters. Note that this function is not strictly admissible but, for k_0 large enough (typically greater than 6), there is no practical difference with a true wavelet (exactly as in the flat case).
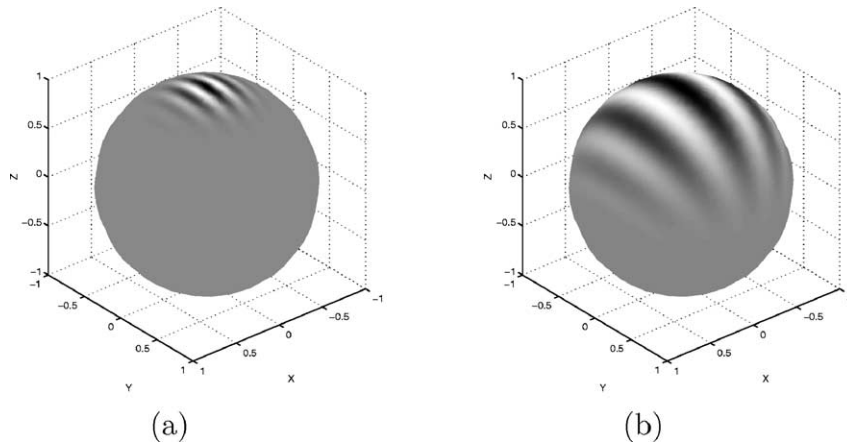
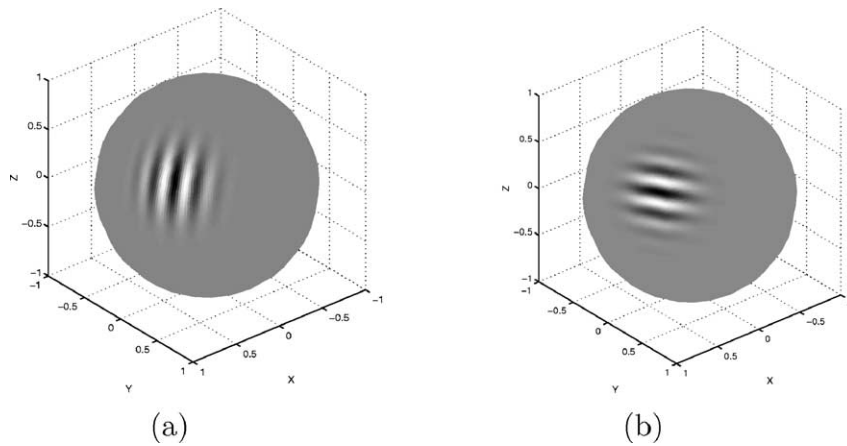Fig. 1. Real part of the spherical Morlet wavelet at scale: (a) $a = 0.03$ and (b) $a = 0.3$.

Fig. 2. Real part of the spherical Morlet wavelet at scale $a = 0.03$ and centered at $(\pi/3, \pi/3)$. (a) $\chi = 0$ and (b) $\chi = \pi/2$.

3. Implementation of the spherical CWT

For a practical implementation of the spherical CWT, the first step is that of discretization. This means finding a suitable grid in the parameter space, so as to allow a fast calculation *and* a good approximation of the continuous theory. As we shall see, the key to the algorithm presented below is to use an FFT in the (periodic) longitude angle φ. We also need some sort of criterion on the grid density for controlling aliasing problems, as indicated already in [3]. More precisely, we have to specify the scale interval in which the spherical wavelet transform makes sense. A possible answer will be suggested in Section 3.2. Then several examples will be discussed, both academic and real life. All the examples are computed with our wavelet toolbox YAWTB/Yet-Another-Wavelet-Toolbox, to be found on the web sites http://www.fyma.ucl.ac.be/projects/yawtb or http://www.yawtb.be.tf.

3.1. Discretization and algorithm

Following an approach similar to that in [25], the first step is to discretize the integral (2.3) on a regular spherical grid $M \times N$

$$\mathcal{G} = \left\{ \left(\theta_t = \frac{\pi}{M} t, \varphi_p = \frac{2\pi}{N} p \right) \,\middle|\, 0 \leqslant t \leqslant M - 1, \, 0 \leqslant p \leqslant N - 1 \right\} \tag{3.1}$$

by a weighted sum (χ and a are fixed throughout)

$$S(\chi, \theta_{t'}, \varphi_{p'}, a) \simeq S[\chi, t', p', a] \tag{3.2}$$

$$= \sum_{\substack{0 \leqslant t \leqslant M-1 \\ 0 \leqslant p \leqslant N-1}} \overline{\psi_{a,\chi,t'}[t, p-p']} s[t, p] w_{tp}, \tag{3.3}$$

where $s[t, p] \equiv s(\theta_t, \varphi_p)$; $\psi_{a,\chi,t'}[t, p-p'] \equiv \psi_{a,\chi,\theta_{t'},0}(\theta_t, \varphi_{p-p'})$; the index of φ is extended to $\mathbb{Z}$ by angular periodicity with the rule $\varphi_{r+N} = \varphi_r$; $w_{tp} = w_t = (2\pi^2/(MN)) \sin \theta_t$ are the weights suggested in [25] for the discretization of the Lebesgue measure on the particular grid $\mathcal{G}$. Notice that other discretization techniques than a plain Riemann sum, as used in (3.3), would be beneficial only if one imposes additional regularity conditions on the signal s. Also, other weights w_{tp} could be chosen to achieve a better approximation of (3.2). An example of a different choice, both for the weights and for the discretization technique, is that of a band-limited spherical function, as considered in [13].

Evaluating the sums in Eq. (3.3) requires MN additions and multiplications for each (t', p'), that is, $M^2 N^2$ operations altogether.

However, an easy simplification can be obtained for the longitudinal coordinates by the use of a Fourier series and the Plancherel formula. Indeed, denoting by

$$\check{h}[t, k] = \sum_{0 \leqslant p \leqslant N-1} h[t, p] \exp\left(-i k p \frac{2\pi}{N}\right), \tag{3.4}$$

the longitudinal Fourier coefficients of a given discrete function h, we obtain

$$S[\chi, t', p', a] = 2\pi \sum_{0 \leqslant t \leqslant M-1} w_t \mathcal{F}[\chi, t', p', a, t] \tag{3.5}$$

with

$$\mathcal{F}[\chi, t', p', a, t] = \sum_{0 \leqslant k \leqslant N-1} \overline{\check{\psi}_{a,\chi,t'}[t, k]} \check{s}[t, k] \exp\left(i k p' \frac{2\pi}{N}\right). \tag{3.6}$$

The quantity $\mathcal{F}$ may be computed with the inverse fast Fourier transform (IFFT), which leads to a reduction of the computational time from $O(M^2 N^2)$ to $O(M^2 N \log N)$. On a grid $\mathcal{G}$ of 256×256, the gain is a factor of 46.

In practice, computing the spherical wavelet transform for a fixed scale a and a fixed orientation χ proceeds along the following steps.

Initialization

- Compute the matrix $\check{\mathbf{s}} = (\check{s}[t, k])_{tk}$ obtained by applying the FFT on each row (*row FFT*) of the original data $\mathbf{s} = (s[t, p])_{tp}$;

For $t' = 0$ to $M - 1$ do

- Compute the matrix $\check{\Psi}_{a,\chi,t'} = (\overline{\check{\psi}_{a,\chi,t'}[t, k]})_{tk}$ deduced from the row FFT of the matrix $\Psi_{a,\chi,t'} = (\overline{\psi_{a,\chi,t'}[t, p]})_{tp}$;
- Compute the product matrix $\check{\mathbf{P}}_{a,\chi,t'} = (\check{s}[t, k] \overline{\check{\psi}_{a,\chi,t'}[t, k]})_{tk}$ and apply the inverse FFT on each of its rows. This yields a matrix $\mathbf{P}_{a,\chi,t'}$ corresponding to the convolution of the rows of $\mathbf{s}$ with the rows of the wavelet $\Psi_{a,t',\chi}$;
- Finally, the t'th row of S is given by

$$S[\chi, t', p', a] = \sum_{0 \leqslant t \leqslant M-1} w_t P_{a,\chi,t'}[t, p'], \quad \text{for } 0 \leqslant p' \leqslant N-1.$$

end.

3.2. Numerical criterion for the scale range

The discretization of the continuous spherical wavelet transform gives rise to a sampling problem. Since the grid $\mathcal{G}$ is fixed, if we contract or dilate too much our wavelet, we obtain a function which is very different from the original ψ. In other words, aliasing occurs and the wavelet is no longer numerically admissible. We may easily understand this phenomenon by studying a dilated wavelet centered on the North Pole.

We have seen in Section 1 that a function $\psi \in L^2(S^2, d\mu)$ is admissible only if it satisfies the zero mean condition (1.4). Approximating the integral by its Riemann sum, we get the quantity

$$\mathcal{C}[\psi] = \sum_{\substack{1 \leqslant t \leqslant M-1 \\ 1 \leqslant p \leqslant N-1}} \frac{\psi(\theta_t, \varphi_p)}{1 + \cos\theta_t} \, w_{tp} \tag{3.7}$$

using the weights w_{tp} defined in the previous section.

Because of the discretization, even if ψ verifies (1.4), it is not necessarily true that $\mathcal{C}[\psi]$ vanishes. However, we may suppose that this quantity is very close to zero when ψ is sampled sufficiently, that is, if the grid $\mathcal{G}$ is fine enough.

However, it is difficult to give a quantitative meaning to the value of $\mathcal{C}[\psi]$. How small is 'very close to zero'? Here is a possible solution to this problem. Since the spherical measure μ and the function $1 + \cos\theta$ are positive, it is clear that

$$\mathcal{C}[\psi] \leqslant \mathcal{C}\big[|\psi|\big] \tag{3.8}$$

for any $\psi \in L^2(S^2, d\mu)$. So we can define a normalized numerical admissibility by

$$\widetilde{\mathcal{C}}[\psi] = \frac{\mathcal{C}[\psi]}{\mathcal{C}[|\psi|]}, \tag{3.9}$$

a quantity always contained in the interval $[-1, 1]$.

We can now give a precise definition of numerical admissibility of a wavelet ψ centered on the North Pole.

Definition 3.1. A spherical wavelet of $L^2(S^2, d\mu)$ is numerically admissible on $\mathcal{G}$ with threshold $p\%$ (or simply $p\%$-admissible on $\mathcal{G}$), if the numerical normalized admissibility (3.9) is smaller than $(100 - p)/100$ in absolute value

$$\big|\widetilde{\mathcal{C}}[\psi]\big| \leqslant \frac{100 - p}{100}. \tag{3.10}$$

As an example, we present in Fig. 3 the behavior of the dilated spherical DOG wavelet, $D_a \psi_{\mathrm{G}}^{(\alpha)} (\alpha = 1.25)$, as a function of $a > 0$, discretized on a 128×128 grid (notice that, in
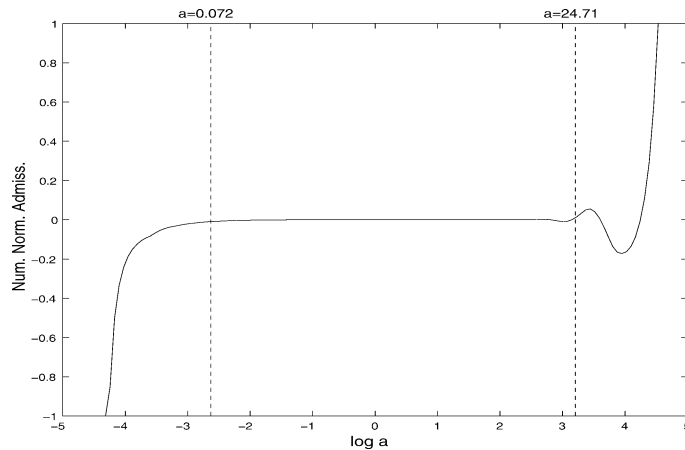

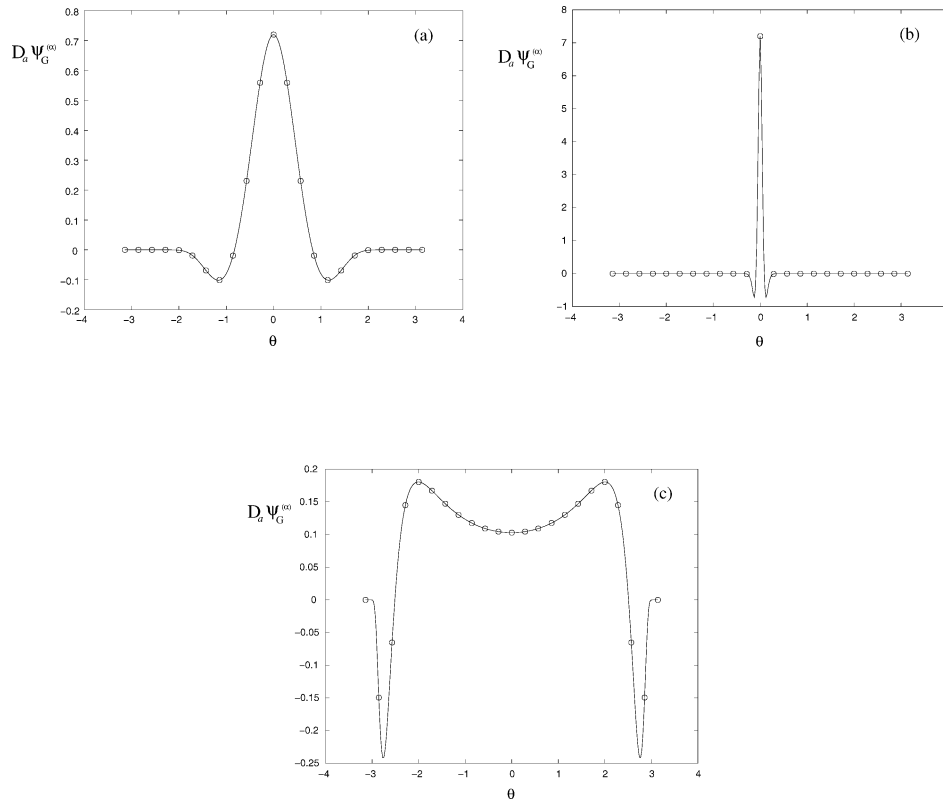Fig. 3. $\widetilde{\mathcal{C}}[D_a \psi_{\mathrm{G}}^{(\alpha)}]$ as a function of $\log a$ for $\alpha = 1.25$.

Fig. 4. Three typical behaviors of $D_a \psi_G^{(\alpha)}$ discretized on a 22×22 grid $\mathcal{G}$. (a) For $a = 0.5$, the sampling is correct. (b) For $a = 0.05$, subsampling occurs, negative parts of $D_a \psi_G^{(\alpha)}$ are completely missed. (c) Subsampling on the negative parts of $D_a \psi_G^{(\alpha)}$ for $a = 3.5$. Notice the minimum at $\theta = 0$.

the flat case, $\alpha = 1.6$ is the value for which the DOG wavelet is almost indistinguishable from the mexican hat).

According to this plot, the wavelet $D_a \psi_G^{(\alpha)}$ is 99%-admissible on the scale interval $a \in [0.072, 24.71]$. The lower limit is due to the fact that, for small a, $D_a \psi_G^{(\alpha)}$ is not sampled enough. The upper limit comes from the subsampling of the area far from the North Pole which, according to the spherical dilation, gets more and more contracted. Figure 4 presents three typical behaviors of $D_a \psi_G^{(\alpha)}$ discretized on a 22 point θ sampling. For $a = 0.5$, the sampling is correct. For $a = 0.05$, that is, below the lower admissibility bound, subsampling occurs, so that negative parts of $D_a \psi_G^{(\alpha)}$ are completely missed. Clearly, this discretized wavelet is no longer admissible. Exactly the same effect was observed long ago in the flat case [3]. The third case, with $a = 3.5$, thus beyond the upper bound, is less intuitive. Here the subsampling takes place for *large* values of θ, that is, close to the South Pole, but the result is the same, the discretized wavelet does not have a zero mean, it is not admissible. In addition, the curve presents a *minimum* at $\theta = 0$. This somewhat unexpected effect is in fact due to the cocycle, as is the dependence of the height on a. Indeed, if one performs the same calculation *without* the cocycle, all curves show a maximum at $\theta = 0$, with the same height. Here again we see that curvature, which requires the presence of the cocycle, has a nontrivial effect.

Two remarks remain to be made about the admissibility and its numerical consequences. Both follow from the obvious fact that choosing polar coordinates effectively breaks the spherical symmetry, by introducing a singularity at the North Pole.

First, the simplified admissibility condition (1.4) is only valid for wavelets which vanish at $\theta = \pi$. So, unlike in the flat case, the simplified admissibility of a mother wavelet ψ does *not* imply that of all the *translated* wavelets $R_\rho \psi$ with ρ in $SO(3)$ (this does not happen, of course, for the full admissibility condition (1.3)).
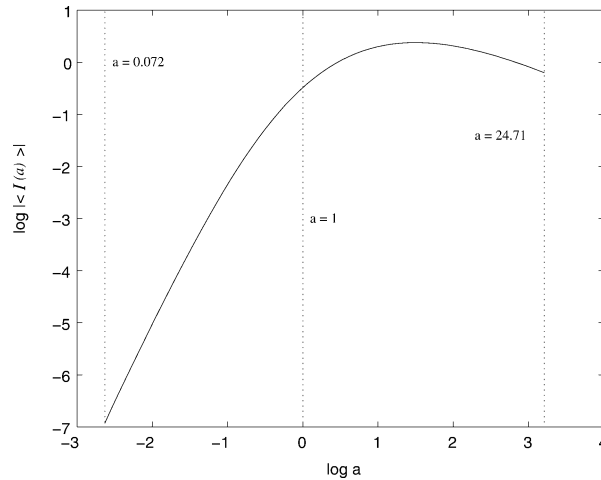
Fig. 5. Mean value $\langle I(a) \rangle$ of the spherical wavelet transform of the unit function ι as a function of the scale a (log–log representation).

Second, the sampling of a wavelet centered on the North Pole is not the same as if it would be centered on an equatorial point. Therefore, given a certain percentage of numerical admissibility for $D_a \psi$, the interval of allowed scales a is not necessarily valid everywhere on the sphere. In other words, we cannot ensure that $R_\rho D_a \psi$ will be sampled finely enough for all the possible $\rho \in SO(3)$.

3.3. Numerical analysis of the unit function

It is instructive to consider the function ι identically equal to 1. In the flat case, this function has a vanishing WT, by the admissibility condition $\int d\vec{x}\, \psi(\vec{x}) = 0$ on the wavelet, but it is not square integrable and thus cannot be reconstructed. In the present case, however, the situation is different. The function ι is square integrable, since the sphere S^2 is compact, but its WT does *not* vanish, because of the presence of the cocycle. Indeed, the function ι is invariant under rotation, but *not* under dilation

$$(D_a \iota)(\theta, \varphi) = \lambda(a, \theta)^{1/2} \not\equiv 1, \tag{3.11}$$

and, therefore,

$$I(\varrho, a) = \langle R_\varrho D_a \psi | \iota \rangle = \langle \psi | D_a \iota \rangle \equiv I(a) = \int_{S^2} d\mu(\omega)\, \overline{\psi(\omega)} \lambda(a, \theta)^{1/2} \neq 0. \tag{3.12}$$

Thus, for fixed a, the WT $I(a)$ of the unit function is constant, and essentially negligible for $a \ll 1$. Significant values appear only for $a > 2$, and these scales are irrelevant for the analysis of signals such as contours. As a consequence, the spherical CWT does have the familiar local filtering effect, provided small scales are considered. This will be confirmed by the examples below. Once again, we see that the CWT is useful only as a *local* analysis.

To get a quantitative estimation of this effect, we present in Fig. 5, the mean value $\langle I(a) \rangle$ of $I(a)$ on the sphere as a function of the scale a. We have to take this average because, in practice, $I(a)$ is not exactly constant due to the gridding artifacts.[3] Variations around this mean are however small, close of 10^{-3}, and essentially constant with scales. We see indeed that, for $a < 0.1$ (this number may depend on the grid used, of course), $\langle I(a) \rangle$ is numerically negligible over the whole sphere, and may be taken as zero to a very good approximation.

---

[3] The density of points on a spherical regular grid is higher at the poles than on the equator.
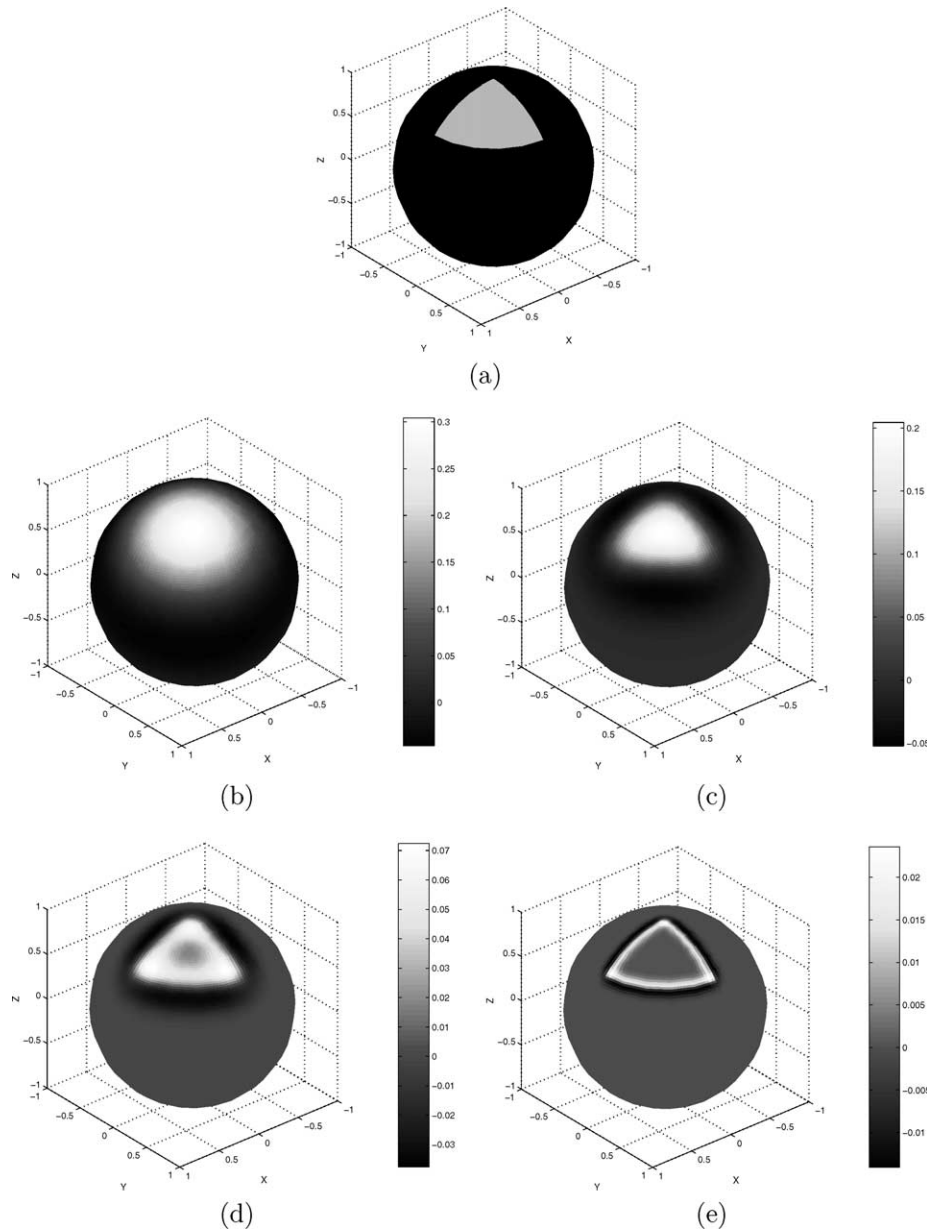
Fig. 6. Spherical wavelet transform of the characteristic function of a spherical triangle with apex at the North Pole, $0° \leqslant \theta \leqslant 50°$, $0° \leqslant \varphi \leqslant 90°$, obtained with the spherical DOG wavelet $\psi_G^{(\alpha)}$ for $\alpha = 1.25$. (a) Original image. The transform is shown at four successive scales: (b) $a = 0.5$; (c) $a = 0.2$; (d) $a = 0.1$; and (e) $a = 0.035$. As expected, it vanishes inside the triangle, and presents a "wall" along the contour, with sharp peaks at each vertex. Notice that the scales are different in the four cases.

3.4. Examples of spherical wavelet transforms

As a first example, we analyze in Fig. 6 an academic picture, namely, (the characteristic function of) a spherical sector on S^2, with one of the corners sitting at the North Pole. The sector is given by $0° \leqslant \theta \leqslant 50°$, $0° \leqslant \varphi \leqslant 90°$ and is discretized on a 128×128 grid in (θ, φ). The wavelet used is again the spherical DOG $\psi_G^{(\alpha)}$, for $\alpha = 1.25$, discretized on the same grid. According to the admissibility analysis presented above (Fig. 3), the wavelet is 95%-admissible on the scale interval $a \in [0.033, 29.27]$. Thus we can evaluate the continuous spherical wavelet transform of this picture for various scales in the allowed range, and we have chosen four successive scales from $a = 0.5$ to $a = 0.035$. Figure 6 shows that the spherical WT behaves here exactly as, in the flat case, the WT of the
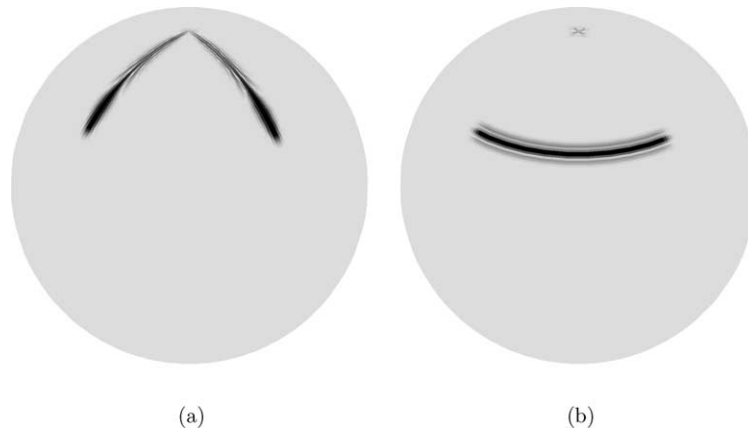
(a)   (b)

Fig. 7. Squared modulus of the spherical wavelet transform of (the characteristic function of) a spherical triangle with apex at the North Pole, $0° \leqslant \theta \leqslant 50°$, $0° \leqslant \varphi \leqslant 90°$, obtained with the spherical Morlet wavelet. $\psi_G^{(\alpha)}$, for $\alpha = 1.25$. (a) For $\chi = 0°$. (b) For $\chi = 90°$. The WT selects the features (here the "walls") oriented along meridians or parallels, according to the value of χ.

characteristic function of a square, as shown in [3]. For large a, the WT sees only the object as a whole, thus allowing to determine its position on the sphere. When a decreases, increasingly finer details appear; in this simple case, only the contour remains, and it is perfectly seen at $a = 0.035$. The transform vanishes in the interior of the triangle, as it should, only the "walls" remain, with a negative value (black) just outside, a zero-crossing right on the boundary and a sharp positive maximum (white) just inside. In addition, each corner gives a neat peak, which is positive, since the corner is convex [3]. Notice that the three corners are alike, so that indeed the poles play no special role in our spherical WT, contrary to what occurs often in the classical spherical analysis based on spherical harmonics [9,10,19,20].

In the second example, Fig. 7, we use the same spherical sector, but defined on a 256×256 spherical grid $\mathcal{G}$. This time, we choose to test the directional sensitivity of the spherical Morlet wavelet, keeping the scale fixed. In the flat case, the wavelet transform responds to different directions as a function of the rotation parameter; here the notion of direction is replaced by that of *orientation with respect to meridians or parallels*. In other words, directions here can be referred to as cardinal points: $\chi = 0°$ corresponds the North–South direction, i.e., meridians, and $\chi = 90°$ to the East–West direction, i.e., parallels. These cardinal points could have been defined in another way, if we remember that we arbitrarily chose to work with the Euler angles in the implementation of our transform.

As a third, real life example, we present in Fig. 8 the wavelet transform of a significant piece of the terrestrial globe, covering Europe, Greenland, and North Africa. As before, we use the spherical DOG wavelet $\psi_G^{(\alpha)}$ for $\alpha = 1.25$. The transforms are shown again at three successive scales, $a = 0.032, 0.016, 0.0082$ (the grid used here is finer than the one used in the previous examples, so that smaller values of a are admissible). As expected, the resolution improves with diminishing a. However, at $a = 0.0082$, the discretization grid used for the computation of the transform coincides with that of the original picture, so that one sees exactly the same artifacts, such as a closed strait of Gibraltar, an unresolved complex Corsica–Sardinia, ragged coastlines, etc. Of course, we cannot hope to *improve* on the resolution of the original! As for the rapidity, the original is a 512×1024 point picture, and each transform takes about one CPU hour on a 400 MHz Digital PC. This is not bad, given the size of the original file. Note that a similar analysis was performed by [21] using the lifting scheme.

4. Wavelet approximations on the sphere

The central theme of approximation theory is the representation of a function by a truncated series expansion into a family of basis functions, for instance, the elements
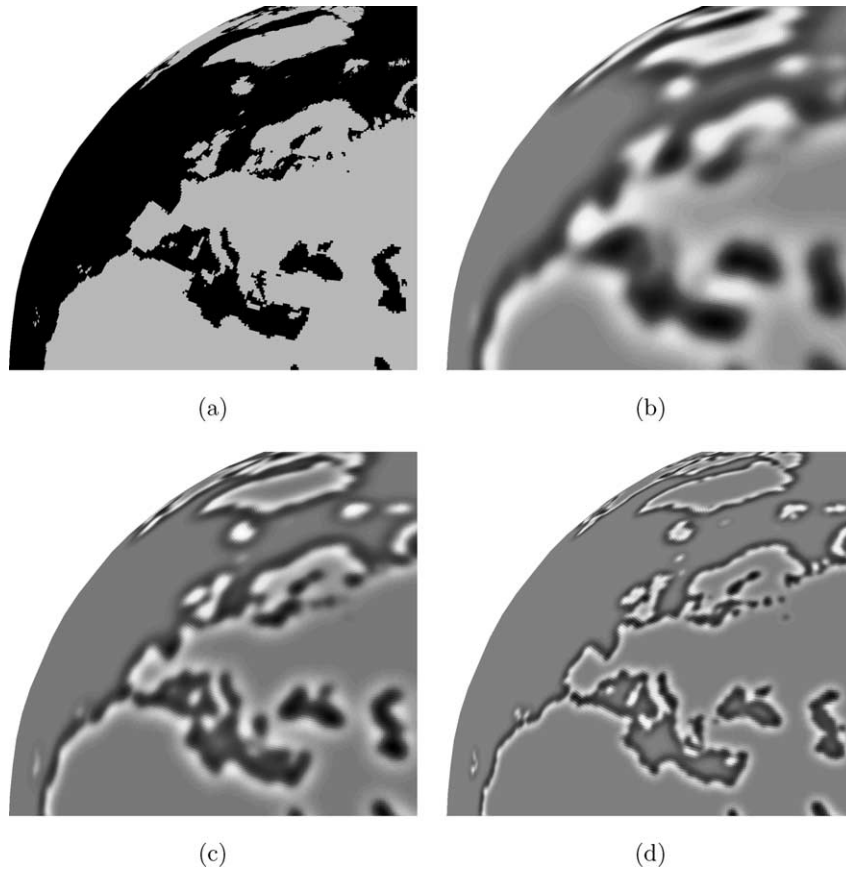
Fig. 8. Spherical wavelet transform of the spherical map of the European area, computed with the spherical DOG wavelet for $\alpha = 1.25$. (a) The original picture; (b) wavelet transform at $a = 0.032$; (c) the same at $a = 0.016$; (d) the same at $a = 0.0082$.

of a frame. Thus, in the flat case, one- or two-dimensional, wavelets are widely used for approximation in various function spaces [15]. The crucial advantage is their multiresolution character, which is optimally adapted to local perturbations. A natural framework is given by the Lebesgue spaces $L^p(\mathbb{R}^n)$, $1 \leqslant p < \infty$. One of the reasons is that approximation is often formulated in terms of convolution with an *approximate identity*, and many useful convolution identities are available in L^p [12,14].

Thus, in order to apply these considerations to the sphere S^2, it is necessary to have a good notion of convolution on S^2. For that purpose, it is useful to represent the sphere as the quotient $SO(3)/SO(2)$, since the convolution machinery extends almost verbatim to locally compact groups, and then partly to homogeneous spaces. For the convenience of the reader, we have collected in the Appendix the main definitions and essential properties of convolution on a locally compact group. In what follows, we will need two different cases. For simplicity, we write $L^2(SO(3)) \equiv L^2(SO(3), d\varrho)$, where $d\varrho$ is the Haar measure on $SO(3)$, and $L^p(S^2) \equiv L^p(S^2, d\mu)$.

- If $f \in L^2(SO(3))$ and $g \in L^1(S^2)$, then $f * g \in L^2(S^2)$ with

$$\|f * g\|_2 \leqslant \|f\|_2 \|g\|_1, \tag{4.1}$$

  where the norms refer to the corresponding spaces.
- If $f \in L^2(S^2)$ and $g \in L^1(S^2)$, their *spherical convolution* is the function on $SO(3)$ defined as

$$(f \,\widetilde{*}\, g)(\varrho) = \int\limits_{S^2} d\mu(\omega)\, f(\varrho^{-1}\omega)g(\omega). \tag{4.2}$$

Then $f \stackrel{\sim}{*} g \in L^2(SO(3), d\varrho)$ and

$$\|f \stackrel{\sim}{*} g\|_2 \leqslant \|f\|_2 \|g\|_1. \tag{4.3}$$

Here, however, we are only interested in functions on the sphere S^2, that is, functions on $SO(3)$ that are $SO(2)$-invariant. In particular, we will deal mostly with axisymmetric functions on S^2, that is, functions of θ alone (such functions are also called *zonal*). Thus, we will focus on elements of $L^2([-1, +1], dt)$, where $t = \cos\theta$, for which the Fourier series reduces to a Legendre expansion

$$\psi(t) = \sum_{l=0}^{\infty} \frac{2l+1}{4\pi} \widehat{\psi}(l) P_l(t), \qquad \widehat{\psi}(l) = 2\pi \int_{-1}^{+1} dt \, P_l(t) \psi(t) = \sqrt{\frac{4\pi}{2l+1}} \, \widehat{\psi}(l, 0).$$

If f is a zonal function, the spherical convolution (4.2) takes a simpler form [10] by the following proposition.

Proposition 4.1. *Let f and g be two measurable functions on S^2. If f is zonal, the spherical convolution of f and g is a function on S^2, which can be written*

$$(f * g)(\omega') = \int_{S^2} d\mu(\omega) \, f(\widehat{\omega}' \cdot \widehat{\omega}) g(\omega), \tag{4.4}$$

where $\widehat{\omega}' \cdot \widehat{\omega}$ is the $\mathbb{R}^3$ scalar product of unit vectors of directions ω' and ω.

Proof. The proof amounts to a straightforward application of harmonic analysis (Fourier series) on S^2. Let us rewrite the argument in the integral (4.2), denoting by $\omega' \equiv \dot{\varrho} \in S^2$ the left coset of $\varrho \in SO(3)$

$$f(\varrho^{-1}\omega') = [U_{\mathrm{qr}}(\varrho)f](\omega') = \sum_{l=0}^{\infty} \sum_{|m| \leqslant l} [U_{\mathrm{qr}}(\varrho)f](l, m) Y_l^m(\omega'),$$

$$= \sum_{l=0}^{\infty} \sum_{|m| \leqslant l} \{\mathcal{D}_{m0}^l(\omega) \hat{f}(l, 0)\} Y_l^m(\omega') \quad \text{(since } f \text{ is zonal)}$$

$$= \sum_{l=0}^{\infty} \hat{f}(l) \sum_{|m| \leqslant l} \overline{Y_l^m(\omega)} Y_l^m(\omega').$$

Then the addition theorem for spherical harmonics yields

$$f(\varrho^{-1}\omega') = \sum_{l=0}^{\infty} \frac{2l+1}{4\pi} \hat{f}(l) P_l(\widehat{\omega}' \cdot \widehat{\omega}) = f(\widehat{\omega}' \cdot \widehat{\omega}). \qquad \square$$

A very useful property of zonal convolution is the *spherical Young inequality*: if $f \in L^p([-1, +1], dt)$ and $g \in L^q(S^2)$, with $1 \leqslant p, q < \infty$, then $f * g \in L^r(S^2)$, with $1/p + 1/q = 1 + 1/r$, and we have [10]

$$\|f * g\|_r \leqslant \|f\|_p \|g\|_q, \quad \text{with } 1/p + 1/q = 1 + 1/r. \tag{4.5}$$

Now we may turn to the approximation problem proper. As in the Euclidean case [14,22], a convenient technique is to perform a convolution with a smoothing kernel, that acts as an approximate identity. For the sake of simplicity, we will only deal with zonal kernels, following mainly [10].

Definition 4.2. Let $\mathcal{K}_\tau$, $\tau \in (0, \tau_0]$, $\tau_0 \in \mathbb{R}_*^+$, be a family of elements of $L^1([-1, +1], dt)$ satisfying $\widehat{\mathcal{K}}_\tau(0) = 1$. The functional $S_\tau[f]$ defined by

$$S_\tau[f] = \mathcal{K}_\tau * f, \quad f \in L^p(S^2), \ 1 \leqslant p < \infty,$$

is called a *singular integral*. It is called an *approximate identity* of $L^p(S^2)$ if

$$\lim_{\tau \to 0, \ \tau > 0} \left\| f - S_\tau[f] \right\|_p = 0, \quad \forall f \in L^p(S^2). \tag{4.6}$$

The following theorem characterizes those spherical kernels which are associated with an approximate identity.

Theorem 4.3. *Let $\{\mathcal{K}_\tau\}$ be a uniformly bounded spherical kernel, that is, there exists a constant M, independent of τ, such that*

$$\int_{-1}^{+1} dt \, |\mathcal{K}_\tau(t)| \leqslant M, \quad \forall \tau \in (0, \tau_o].$$

Then the associated singular integral is an approximate identity of $L^p(S^2)$ if and only if

$$\lim_{\tau \to 0, \ \tau > 0} \widehat{\mathcal{K}}_\tau(n) = 1, \quad \forall n \geqslant 0. \tag{4.7}$$

A proof may be found in [10]. A particularly interesting case is given by positive definite kernels. In this case, since $|P_l(t)| \leqslant 1$, $\{\mathcal{K}_\tau\}$ is uniformly bounded, with bound $M = \sup_{\tau \in (0, \tau_0]} \widehat{\mathcal{K}}_\tau(0)$.

The following theorem gives a nice characterization of approximate identities associated with positive kernels.

Theorem 4.4. *Let $\{\mathcal{K}_\tau\}$, $\tau \in (0, \tau_o]$, be a positive kernel associated to a singular integral of $L^p(S^2)$. Then each of the following conditions is equivalent to (4.6) and (4.7), which means that $\{\mathcal{K}_\tau\}$ is the kernel of an approximate identity*:

(i) $\lim_{\tau \to 0, \ \tau > 0} \widehat{\mathcal{K}}_\tau(0) = 1$,
(ii) $\lim_{\tau \to 0, \ \tau > 0} \int_{-1}^{\delta} dt \, \mathcal{K}_\tau(t) = 0$, $\delta \in (-1, +1)$.

It is important to notice that the second condition is a constraint on the localization of the kernel. Approximate identities are a very useful tool for harmonic analysis on the sphere and many applications can be found in [10].

We can now reformulate the results of Section 1 in the language of approximate identities on the sphere. This is a very interesting way of handling functions on the sphere, because it allows to represent information by means of localized, and hierarchically organized, coefficients. With such a representation, a local modification of the function would only result in a slight local perturbation of the original coefficients, a definite advantage over Fourier series.

Many examples of approximate identities are given in [10]. In general, they are based on families of kernels indexed by a parameter which behaves like a dilation. Such are, for instance, the Abel–Poisson kernel,

$$\mathcal{Q}_\tau(t) = \frac{1}{4\pi} \frac{1 - \tau^2}{(1 + \tau^2 - 2\tau t)^{3/2}} = \sum_{l=0}^{\infty} \frac{2l + 1}{4\pi} \tau^l P_l(t), \quad \tau \in (0, 1),$$

and the Gauss kernel,

$$\mathcal{G}_\tau(t) = \sum_{l=0}^{\infty} \frac{2l + 1}{4\pi} e^{-l(l+1)\tau} P_l(t), \quad \tau \in \mathbb{R}_*^+.$$

Since dilation is introduced directly as a parameter in those kernels, there is no unique way of generating approximate identities, as in $\mathbb{R}^n$. But this problem disappears naturally if one uses the spherical dilation. However, we have to modify the dilation operator and adapt it to the L^1 environment. Using the notation of Section 1, we define, instead of D_a, as given in (1.2), the new dilation operator

$$\left(D^a f \right)(\omega) \equiv f^a(\omega) = \lambda(a, \theta) f(\omega_{1/a}), \tag{4.8}$$

and this operator clearly conserves the L^1 norm. Notice that the situation is more complicated here than in the flat case. There, indeed, changing the dilation operator from L^2 to L^1 simply amounts to change the power of a in front of the transform [6]. Here, one replaces the factor $\lambda(a, \theta)^{1/2}$ by its square $\lambda(a, \theta)$, but this modifies the CWT itself in a nontrivial way. In particular, the admissibility condition (1.3) becomes

$$\frac{8\pi^2}{2l+1} \sum_{|m| \leqslant l} \int_0^\infty \frac{da}{a} \left| \widehat{\psi}^a(l, m) \right|^2 < c. \tag{4.9}$$

The following result, the equivalent of Proposition 3.7 of [6], shows that our new dilation operator does not change the mean of a function.

Proposition 4.5. *If $\psi \in L^1(S^2)$, then*

$$\int_{S^2} d\mu(\omega) \, \psi^a(\omega) = \int_{S^2} d\mu(\omega) \, \psi(\omega). \tag{4.10}$$

The proof reduces to a simple change of variables, followed by using the cocycle relation

$$\lambda(a^{-1}, \theta)\lambda(a, \theta_a) = \lambda(1, \theta) = 1.$$

Acting with this dilation on a suitable function, one can now construct easily an approximate identity, as shown in the next proposition.

Proposition 4.6. *Let $f \in C([-1, +1])$ satisfying $\hat{f}(0) = 1$. Then the family $\{f^a \equiv D^a f, a > 0\}$, is the kernel of an approximate identity.*

Proof. The family $\{f^a\}$, $a \in (0, 1]$, is uniformly bounded because

$$\int_{-1}^{+1} dt \, \left| f^a(t) \right| = \| f \|_1.$$

It thus remains to verify that

$$\lim_{a \to 0, \, a > 0} \widehat{f^a}(l) = 1.$$

With the following change of variables:

$$t' = \frac{(a^2 + 1)t + (a^2 - 1)}{(a^2 - 1)t + (a^2 + 1)},$$

and using the cocycle law, for all $a \in (0, 1]$, we find

$$\lim_{a \to 0, \, a > 0} \widehat{f^a}(l) = \lim_{a \to 0, \, a > 0} \int_{-1}^{+1} dt' \, P_l \left(\frac{(1 + a^2)t' + (1 - a^2)}{(1 - a^2)t' + (1 + a^2)} \right) f(t').$$

The integrand is bounded:

$$\left| P_l \left(\frac{(1 + a^2)t' + (1 - a^2)}{(1 - a^2)t' + (1 + a^2)} \right) f(t') \right| \leqslant \max_{t \in [-1, +1]} \left| f(t) \right|,$$

and since

$$\lim_{a \to 0, \, a > 0} P_l \left(\frac{(1 + a^2)t' + (1 - a^2)}{(1 - a^2)t' + (1 + a^2)} \right) = 1,$$

we finally have

$$\lim_{a \to 0, \, a > 0} \widehat{f^a}(l) = \hat{f}(0) = 1,$$
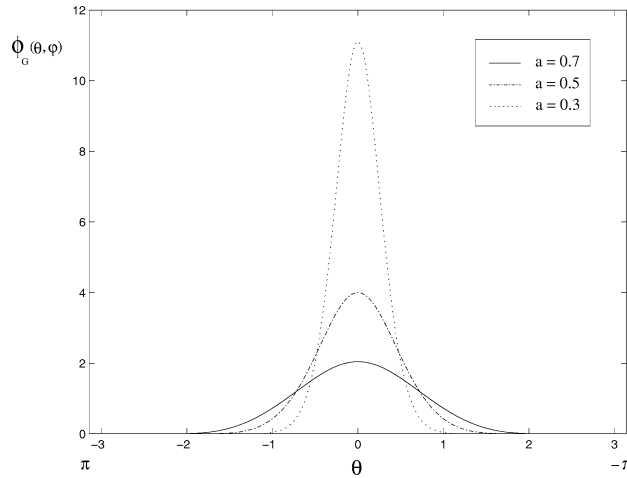
which gives the result. $\square$

Fig. 9. Kernel of an approximate identity obtained by dilating a Gaussian mother function with scaling factor $a = 0.7$ (continuous), 0.5 (dashed), and 0.3 (dotted).

This technique is applied in Fig. 9 to a zonal function of Gaussian shape, namely the mother wavelet of the spherical DOG wavelet, $\phi_G(\theta, \varphi) = \exp(-\tan^2(\theta/2))$, $\theta \in [-\pi, \pi]$. One clearly sees how dilation localizes the kernel better and better as $a \to 0$.

In the L^1 formalism, we recall from [6] that the necessary condition for admissibility becomes a genuine zero mean condition, exactly as in the flat case

$$\widehat{\psi}(0, 0) = \frac{1}{\sqrt{4\pi}} \int\limits_{S^2} d\mu(\theta, \varphi)\, \psi(\theta, \varphi) = 0, \tag{4.11}$$

and, therefore, by Proposition 4.5, $\widehat{\psi^a}(0, 0) = 0$, $\forall a > 0$.

Correspondingly, the difference wavelet $\psi_\phi^{(\alpha)}$ given in (1.5) is replaced by

$$\widetilde{\psi}_\phi^{(\alpha)}(\theta, \varphi) = \phi(\theta, \varphi) - D^\alpha \phi(\theta, \varphi), \quad \alpha > 1.$$

Now, combining the modified dilation operator D^a with the usual rotation operator R_ϱ, we define a new set of spherical wavelets, starting from an admissible ψ, namely, $\psi_\varrho^a \equiv R_\varrho D^a \psi = R_\varrho \psi^a$. Accordingly, we redefine as follows the spherical wavelet transform of a signal $s \in L^2(S^2)$:

$$\widetilde{S}_\psi(\varrho, a) = \int\limits_{S^2} d\mu(\omega)\, \overline{\psi_\varrho^a(\omega)}\, s(\omega). \tag{4.12}$$

In particular, if the wavelet ψ is zonal, we get

$$\widetilde{S}_\psi(\omega, a) = \int\limits_{S^2} d\mu(\omega')\, \overline{\psi^a\big(\widehat{\omega} \cdot \widehat{\omega'}\big)}\, s(\omega'). \tag{4.13}$$

We can now state our main result, namely that the spherical CWT admits a reconstruction formula, valid in the strong L^2 topology, exactly as the usual CWT in $\mathbb{R}^n$. Actually, the formula holds in any strong L^p topology, for $1 \leqslant p < \infty$. As in the flat case [8,18,23], we may distinguish between a bilinear and a linear formalism (the latter being a limiting case of the former). But there is a crucial difference. In the flat case, it is advantageous, but not compulsory, to treat the large scales or low frequencies separately, in terms of a scaling function (in the context of the so-called *infinitesimal multiresolution analysis*). Here, however, we are *forced* to do it. The reason is that, geometrically, only small scales are relevant and lead to the expected filtering behavior, as discussed in Section 3.3. We arbitrarily choose $a = a_o$ as reference scale and define the scales $a > a_o$ as large (we could, for instance, put $a_o = 1$).

Let us begin with the bilinear analysis. Given a wavelet $\psi \in L^1(S^2)$, we define the corresponding *scaling function* $\Phi \equiv \Phi^{(a_o)}$ by its Fourier coefficients

$$\left|\widehat{\Phi}(l, m)\right|^2 = \int\limits_{a_o}^{\infty} \frac{\mathrm{d}a}{a} \left|\widehat{\psi^a}(l, m)\right|^2, \quad l \geqslant 1, \tag{4.14}$$

$$\left|\widehat{\Phi}(0, 0)\right|^2 = \frac{1}{8\pi^2}; \tag{4.15}$$

the integral in (4.14) converges in virtue of the admissibility condition (4.9) satisfied by ψ. Of course, (4.14) does not define the function Φ uniquely. We can, for instance, assume in addition that $\widehat{\Phi}(l, m) \geqslant 0$, $\forall l, m$, as in [10].

Corresponding to (4.12), we define the *large scale part* of a signal s as

$$\widetilde{\Sigma}_\Phi(\varrho, a_o) = \int\limits_{S^2} \mathrm{d}\mu(\omega) \, \overline{\Phi_\varrho^{(a_o)}(\omega)} \, s(\omega), \tag{4.16}$$

where we have put $\Phi_\varrho^{(a_o)}(\omega) \equiv \Phi^{(a_o)}(\varrho^{-1}\omega)$.

Theorem 4.7 (Bilinear analysis). *Let $\psi \in L^1(S^2)$ be a wavelet and let $\Phi \equiv \Phi^{(a_o)}$, $a_o > 0$, denote the associated scaling function. Assume the following two conditions are satisfied:*

- *for all $l = 1, 2, \ldots,$*

$$\frac{8\pi^2}{2l + 1} \sum\limits_{|m| \leqslant l} \int\limits_0^\infty \frac{\mathrm{d}a}{a} \left|\widehat{\psi^a}(l, m)\right|^2 = 1, \tag{4.17}$$

- *for all $\epsilon \in (0, a_o)$, there is a constant $M > 0$, independent of ϵ, such that*

$$\int\limits_\epsilon^{a_o} \frac{\mathrm{d}a}{a} \left\|\psi^a\right\|^2 \leqslant M. \tag{4.18}$$

Then, for all $s \in L^2(S^2)$, we have the equality

$$s = \int\limits_0^{a_o} \frac{\mathrm{d}a}{a} \int\limits_{SO(3)} \mathrm{d}\varrho \, \widetilde{S}_\psi(\varrho, a) \, \psi_\varrho^a + \int\limits_{SO(3)} \mathrm{d}\varrho \, \widetilde{\Sigma}_\Phi(\varrho, a_o) \Phi_\varrho^{(a_o)}, \tag{4.19}$$

where $\widetilde{S}_\psi$ is the spherical CWT of s with respect to the wavelet ψ, $\widetilde{\Sigma}_\Phi$ is the large scale part of s and the integral is understood in the strong sense in $L^p(S^2)$, $1 \leqslant p < \infty$.

Proof. We consider the first term in (4.19). Since $\psi \in L^1(S^2)$ and $s \in L^2(S^2)$, Young's convolution inequality (4.2) shows that $\widetilde{S}_\psi \in L^2(SO(3))$. As in the flat case [23], we define the infinitesimal detail at scale a

$$d^{(a)}(\omega) = \int\limits_{SO(3)} \mathrm{d}\varrho \, \widetilde{S}_\psi(\varrho, a) \psi_\varrho^a(\omega).$$

This is a convolution on $SO(3)$ and Young's inequality (4.1) shows that $d^{(a)} \in L^2(S^2)$.

Explicitly, we have

$$d^{(a)}(\omega) = \int\limits_{S^2} \mathrm{d}\mu(\omega') \, s(\omega') \int\limits_{SO(3)} \mathrm{d}\varrho \, \overline{\psi^a(\varrho^{-1}\omega')} \, \psi^a(\varrho^{-1}\omega). \tag{4.20}$$

As in the proof of Proposition 4.1, we use the relation

$$\psi^a(\varrho^{-1}\omega') = \sum\limits_{l=0}^\infty \sum\limits_{|m| \leqslant l} \sum\limits_{|n| \leqslant l} \mathcal{D}_{mn}^l(\varrho) \widehat{\psi^a}(l, n) Y_l^m(\omega'), \tag{4.21}$$

to find

$$d^{(a)}(\omega) = \int\limits_{S^2} d\mu(\omega')\, s(\omega') \sum_{\substack{lmn \\ l'm'n'}} \overline{Y_l^m(\omega')}\, Y_{l'}^{m'}(\omega)\, \overline{\widehat{\psi^a}(l, n)}\, \widehat{\psi^a}(l', n')$$

$$\times \int\limits_{SO(3)} d\varrho\, \overline{\mathcal{D}_{mn}^l(\varrho)}\, \mathcal{D}_{m'n'}^{l'}(\varrho).$$

Using the orthogonality of Wigner functions and the addition theorem for spherical harmonics, this gives

$$d^{(a)}(\omega) = 2\pi \int\limits_{S^2} d\mu(\omega')\, s(\omega') \sum_{l=0}^{\infty} \sum_{|m| \leqslant l} P_l(\widehat{\omega} \cdot \widehat{\omega}')\big|\widehat{\psi^a}(l, m)\big|^2.$$

Now consider the following expression:

$$s_\epsilon^{(a_o)}(\omega) = \int\limits_\epsilon^{a_o} \frac{da}{a} d^{(a)}(\omega) = 2\pi \int\limits_{S^2} d\mu(\omega') s(\omega') \int\limits_\epsilon^{a_o} \frac{da}{a} \sum_{l=0}^{\infty} \sum_{|m| \leqslant l} P_l(\widehat{\omega} \cdot \widehat{\omega}')\big|\widehat{\psi^a}(l, m)\big|^2.$$

In virtue of condition (4.18), the double summation on the right-hand side of this equation is absolutely and uniformly convergent, since it is majorized by

$$\int\limits_\epsilon^{a_o} \frac{da}{a} \sum_{l=0}^{\infty} \sum_{|m| \leqslant l} \big|\widehat{\psi^a}(l, m)\big|^2 = \int\limits_\epsilon^{a_o} \frac{da}{a} \|\psi^a\|^2.$$

Now let us introduce the quantity

$$\mathcal{K}_\epsilon^{(a_o)}(t) = 2\pi \sum_{l=0}^{\infty} \sum_{|m| \leqslant l} \left(\int\limits_\epsilon^{a_o} \frac{da}{a} \big|\widehat{\psi^a}(l, m)\big|^2 \right) P_l(t),$$

so that

$$s_\epsilon^{(a_o)} = \mathcal{K}_\epsilon^{(a_o)} * s.$$

By (4.18), we see that $\mathcal{K}_\epsilon^{(a_o)} \in L^1([-1, +1])$, for all $0 < \epsilon \leqslant a_o$, and $\|\mathcal{K}_\epsilon^{(a_o)}\|_1 \leqslant 2\pi M$.

Next, we show in the same way that the second term in (4.19) equals $\mathcal{H}^{(a_o)} * s$, where

$$\mathcal{H}^{(a_o)}(t) = 2\pi \sum_{l=0}^{\infty} \sum_{|m| \leqslant l} \big|\widehat{\Phi}(l, m)\big|^2 P_l(t).$$

Again, $\mathcal{H}^{(a_o)} \in L^1([-1, +1])$. Finally, we define the kernel $\mathcal{K}_\epsilon = \mathcal{K}_\epsilon^{(a_o)} + \mathcal{H}^{(a_o)}$, which also belongs to $L^1([-1, +1])$. Condition (4.18) shows that $\mathcal{K}_\epsilon$ is a uniformly bounded kernel. In addition, from (4.17) and the definition (4.14)–(4.15) of $\widehat{\Phi}(l, m)$, we deduce the following constraint on its Legendre coefficients:

$$\lim_{\epsilon \to 0} \widehat{\mathcal{K}_\epsilon}(l) = \frac{8\pi^2}{2l+1} \sum_{|m| \leqslant l} \left(\int\limits_0^{a_o} \frac{da}{a} \big|\widehat{\psi^a}(l, m)\big|^2 + \big|\widehat{\Phi}(l, m)\big|^2 \right)$$

$$= \begin{cases} \dfrac{8\pi^2}{2l+1} \displaystyle\sum_{|m| \leqslant l} \int\limits_0^{\infty} \frac{da}{a} \big|\widehat{\psi^a}(l, m)\big|^2 = 1, & l \geqslant 1, \\[2ex] 8\pi^2 \big|\widehat{\Phi}(0, 0)\big|^2 = 1, & l = 0. \end{cases}$$

Then Theorem 4.3 shows that $\mathcal{K}_\epsilon$ is the kernel of an approximate identity, which proves the existence of the strong limit in $L^2(S^2)$

$$\lim_{\epsilon \to 0} (\mathcal{K}_\epsilon * s) = s. \qquad \square$$

As a check of the reconstruction formula (4.19), let us consider the unit function ι. Contrary to the case of the L^2 formalism, the L^1-normalized CWT of ι vanishes identically, as a consequence of Proposition 4.5

$$\widetilde{I}_\psi(\varrho, a) = \int\limits_{S^2} d\mu(\omega)\, \overline{\psi^a(\omega)} = \int\limits_{S^2} d\mu(\omega)\, \overline{\psi(\omega)} = 0.$$

Hence only the second term, the large scale part, subsists in (4.19). Using again the expansion (4.21), we find successively

$$\widetilde{I}_\Phi(\varrho, a_o) = \int\limits_{S^2} d\mu(\omega)\, \overline{\Phi(\varrho^{-1}\omega)} = \overline{\widehat{\Phi}(0,0)},$$

and, for (4.19),

$$\iota(\omega) = \overline{\widehat{\Phi}(0,0)} \int\limits_{SO(3)} d\varrho\, \overline{\Phi(\varrho^{-1}\omega)} = 8\pi^2 |\widehat{\Phi}(0,0)|^2 = 1.$$

This result shows that the large scale part of a signal must be treated separately, because constant functions on the sphere are square integrable, and hence must be reconstructible, although their CWT vanishes identically. In practice, of course, large scales should be irrelevant, since wavelet analysis is local, and we expect the second term in (4.19) to be numerically negligible (that is, one must choose a_o large enough for this to be true).

Theorem 4.7 applies, in particular, to a zonal wavelet. The only change is the parameter space of the spherical CWT which takes the form of the product $S^2 \times \mathbb{R}_*^+$, with the measure $a^{-1}\, da\, d\mu(\omega)$. A further simplification yet is to consider a singular reconstruction wavelet and build a framework similar to the Morlet linear analysis. As in the bilinear case, we begin by defining, through its Legendre coefficients, a scaling function $\phi \equiv \phi^{(a_o)}$ that takes care of the large scales

$$\widehat{\phi}(l) = \int\limits_{a_o}^{\infty} \frac{da}{a}\, \widehat{\psi^a}(l), \quad l \geqslant 1, \tag{4.22}$$

$$\widehat{\phi}(0) = 1. \tag{4.23}$$

The corresponding large part of a signal s is then

$$\tilde{\sigma}_\phi(\omega, a_o) = \int\limits_{S^2} d\mu(\omega')\, \overline{\phi(\widehat{\omega} \cdot \widehat{\omega}')}\, s(\omega'). \tag{4.24}$$

In these notations, the linear reconstruction formula is given by the following theorem.

Theorem 4.8 (Linear analysis). *Let $\psi \in L^1(S^2)$ be a zonal wavelet satisfying the following two conditions*:

- *for all $l = 1, 2, \ldots$,*

$$\int\limits_0^\infty \frac{da}{a}\, \widehat{\psi^a}(l) = 1, \tag{4.25}$$

- *for all $\epsilon \in (0, a_o)$,*

$$\sum_{l=0}^\infty \frac{2l+1}{4\pi} \int\limits_\epsilon^{a_o} \frac{da}{a}\, \widehat{\psi^a}(l) < \infty. \tag{4.26}$$

Then, for all $s \in L^2(S^2)$, we have the equality

$$s(\omega) = \int\limits_0^{a_o} \frac{da}{a}\, \widetilde{S}_\psi(\omega, a) + \tilde{\sigma}_\phi(\omega, a_o),$$

the integral being again understood in the strong sense in L^p, $1 \leqslant p < \infty$.

Proof. The same arguments as in the proof of Theorem 4.7 show that the partial sum

$$s_\epsilon^{(a_o)}(\omega) = \int_\epsilon^{a_o} \frac{da}{a} \, \widetilde{S}_\psi(\omega, a)$$

belongs to $L^2(S^2)$. Expanding this expression and adding the large scale term, we find

$$s_\epsilon(\omega) = \int_{S^2} d\mu(\omega') \int_\epsilon^{a_o} \frac{da}{a} \, \overline{\psi^a(\widehat{\omega} \cdot \widehat{\omega'})} \, s(\omega') + \tilde{\sigma}_\phi(\omega, a_o)$$

$$= \int_{S^2} d\mu(\omega') \, s(\omega') \left(\int_\epsilon^{a_o} \frac{da}{a} \, \overline{\psi^a(\widehat{\omega} \cdot \widehat{\omega'})} + \overline{\phi(\widehat{\omega} \cdot \widehat{\omega'})} \right)$$

$$= \int_{S^2} d\mu(\omega') \, s(\omega') \sum_{l=0}^\infty \frac{2l+1}{4\pi} \left(\int_\epsilon^{a_o} \frac{da}{a} \, \overline{\widehat{\psi^a}(l)} + \overline{\widehat{\phi}(l)} \right) P_l(\widehat{\omega} \cdot \widehat{\omega'})$$

$$= (\kappa_\epsilon * s)(\omega),$$

where we have used (4.26) and set

$$\kappa_\epsilon(t) = \sum_{l=0}^\infty \frac{2l+1}{4\pi} \left(\int_\epsilon^{a_o} \frac{da}{a} \, \overline{\widehat{\psi^a}(l)} + \overline{\widehat{\phi}(l)} \right) P_l(t).$$

The Legendre coefficients of this kernel are

$$\hat{\kappa}_\epsilon(l) = \int_\epsilon^{a_o} \frac{da}{a} \, \overline{\widehat{\psi^a}(l)} + \overline{\widehat{\phi}(l)}.$$

As in the proof of Theorem 4.7, we deduce from condition (4.25) that $\lim_{\epsilon \to 0} \hat{\kappa}_\epsilon(l) = 1$, $\forall l = 0, 1, \ldots$. Thus we have again an approximate identity, which allows us to conclude that

$$\lim_{\epsilon \to 0} \|s - \kappa_\epsilon * s\|_p = 0. \qquad \square$$

The conclusion of this analysis is that our spherical CWT, with the modified dilation operator D^a, leads to the same approximation scheme as that developed by Freeden [10,11]. Moreover, the present approach has the additional advantage of giving a clear geometric meaning to the approximation parameter a. By the same token, it intuitively explains the validity of the Euclidean limit established in [6]. Indeed, taking $a \to 0$ means going to the pointwise limit where curvature becomes unimportant, that is, going to the tangent plane and recovering the flat CWT.

Acknowledgment

Appendix A. Convolution on a locally compact group

Convolution of functions on a locally compact group is a well-defined operation that shares many properties with its well-known Euclidean counterpart. It is defined as follows

Definition A.1 (Group convolution). Let G be a locally compact group with left Haar measure $\mathrm{d}x$, normalized to 1, and let $f, g : G \to \mathbb{C}$ be two measurable functions. The convolution product of f and g is defined a.e. by the integral:

$$(f * g)(x) \equiv \int_G f(xy)g(y^{-1}) \, \mathrm{d}y = \int_G f(y)g(y^{-1}x) \, \mathrm{d}y. \tag{A.1}$$

When G is a commutative group, one has $f * g = g * f$. In general, however, convolution is a noncommutative operation and we have the following relations:

$$(f * g)(x) = \int_G f(xy^{-1})g(y)\Delta(y^{-1}) \, \mathrm{d}y,$$

where $\Delta(x)$ is the modular function on G.

One of the most interesting properties of the convolution integral is its regularizing effect on L^p elements. This is embodied in a number of inequalities, which we shall use often in the sequel. Actually, they all stem from the following general statement, analog to [14, Theorem 4.2], itself a generalization of [12, Proposition V.4.6].

Proposition A.2 (Young's inequality). *Let G be a locally compact group with left Haar measure $\mathrm{d}x$. Let $p, q, r \geqslant 1$ and $1/p + 1/q + 1/r = 2$. Let $f \in L^p(G, \mathrm{d}x)$, $g \in L^q(G, \mathrm{d}x)$, and $h \in L^r(G, \mathrm{d}x)$. Then*

$$\left| \int_G (f * g)(x)h(x) \, \mathrm{d}x \right| = \left| \int_G \int_G f(y)g(y^{-1}x)h(x) \, \mathrm{d}x \, \mathrm{d}y \right|$$
$$\leqslant \|f\|_p \|g\|_q \|h\|_r. \tag{A.2}$$

Equivalently,

$$\|f * g\|_r \leqslant \|f\|_p \|g\|_q, \quad \text{with } \frac{1}{p} + \frac{1}{q} = 1 + \frac{1}{r}. \tag{A.3}$$

Proof. We follow closely the proof of [14, Theorem 4.2], assuming that f, g, h are real and nonnegative. Rewrite the left-hand side of (A.2) as

$$I = \int_G \int_G \alpha(x, y)\beta(x, y)\gamma(x, y) \, \mathrm{d}x \, \mathrm{d}y,$$

with

$$\alpha(x, y) = f(y)^{p/r'} g(y^{-1}x)^{q/r'},$$
$$\beta(x, y) = g(y^{-1}x)^{q/p'} h(x)^{r/p'}, \quad (1/p + 1/p' = 1, \text{ etc.})$$
$$\gamma(x, y) = f(y)^{p/q'} h(x)^{r/q'}.$$

Noting that $1/p' + 1/q' + 1/r' = 1$, we get from Hölder's inequality for three functions [14] $|I| \leqslant \|\alpha\|_{r'} \|\beta\|_{p'} \|\gamma\|_{q'}$. Then

$$\|\alpha\|_{r'}^{r'} = \int_G \int_G f(y)^p g(y^{-1}x)^q \, \mathrm{d}x \, \mathrm{d}y = \int_G \int_G f(y)^p g(x)^q \, \mathrm{d}x \, \mathrm{d}y = \|f\|_p^p \|g\|_q^q,$$

where we have replaced x by yx and used the left invariance of the Haar measure $\mathrm{d}x$ (the integrals may be interchanged by Fubini's theorem). The same change of variables yields $\|\beta\|_{p'}^{p'} = \|g\|_q^q \|h\|_r^r$ and trivially $\|\gamma\|_{q'}^{q'} = \|f\|_p^p \|h\|_r^r$. Putting the three results together then yields the right-hand side of (A.2). As for (A.3), it is a mere restatement of (A.2). □

The result of Proposition A.2 extends to homogeneous spaces, as mentioned already in [12, Section V.4] for the particular case $p = 1$, $r = p'$.

Proposition A.3 (Young's inequality on homogeneous spaces). *Let G be a locally compact group with left Haar measure* dx, H *a closed subgroup such that the quotient space* G/H *has the left invariant measure* $d\omega$. *Let* $p, q, r \geqslant 1$ *and* $1/p + 1/q + 1/r = 2$. *Let* $f \in L^p(G, dx)$, $g \in L^q(G/H, d\omega)$, *and* $h \in L^r(G/H, d\omega)$. *Then*

$$\left| \int_{G/H} (f * g)(\omega) h(\omega) \, d\omega \right| = \left| \int_{G/H} \int_G f(y) g(y^{-1}\omega) h(\omega) \, d\omega \, dy \right|$$

$$\leqslant \|f\|_p \|g\|_q \|h\|_r. \tag{A.4}$$

Equivalently, $f \in L^p(G, dx)$, $g \in L^q(G/H, d\omega)$ *implies* $f * g \in L^r(G/H, d\omega)$ *with* $1/p + 1/q = 1 + 1/r$ *and*

$$\|f * g\|_r \leqslant \|f\|_p \|g\|_q. \tag{A.5}$$

Similarly, $g \in L^q(G/H, d\omega)$, $h \in L^r(G/H, d\omega)$ *implies* $g \widetilde{*} h \in L^p(G, dx)$, *with* $1/q + 1/r = 1 + 1/p$, *and*

$$\|g \widetilde{*} h\|_p \leqslant \|g\|_q \|h\|_r, \tag{A.6}$$

where we have defined the spherical convolution as

$$(g \widetilde{*} h)(y) = \int_{G/H} g(y^{-1}\omega) h(\omega) \, d\omega. \tag{A.7}$$

Proof. The proof is essentially the same, replacing $x \in G$ by $\omega \in G/H$, up to the inequality $|I| \leqslant \|\alpha\|_{r'} \|\beta\|_{p'} \|\gamma\|_{q'}$. For the first factor, we get

$$\|\alpha\|_{r'}^{r'} = \int_{G/H} \int_G f(y)^p g(y^{-1}\omega)^q \, d\omega \, dy = \int_{G/H} \int_G f(y)^p g(\omega)^q \, d\omega \, dy = \|f\|_p^p \|g\|_q^q,$$

where we have replaced ω by $y\omega$ and used the left invariance of the Haar measure $d\omega$. For the second factor, we have to proceed differently. We have

$$\|\beta\|_{p'}^{p'} = \int_{G/H} \int_G g(y^{-1}\omega)^q e(y) h(\omega)^r \, d\omega \, dy,$$

where $e(y) = 1$, $\forall y \in G$. Obviously, $e \in L^1(G, dx)$ and $g^q \in L^1(G/H, d\omega)$, hence $g^q * e \in L^1(G/H, d\omega)$, with $\|g^q * e\|_1 \leqslant \|e\|_1 \|g^q\|_1 = \|g\|_q^q$. From this, we get, by the Schwarz inequality,

$$\|\beta\|_{p'}^{p'} = \int_{G/H} (g^q * e)(\omega) h(\omega)^r \, d\omega \leqslant \|g^q * e\|_1 \|h^r\|_1 = \|g\|_q^q \|h\|_r^r.$$

The rest is unchanged. $\quad\square$

Note that sharper constants, smaller than 1, may be put in the upper bounds on the right-hand side of all the inequalities, as shown in detail for $\mathbb{R}^n$ in [14]. In the text, we use these inequalities for $G = SO(3)$, $G/H = SO(3)/SO(2) = S^2$, under the following continuous inclusions:

$$L^2(SO(3), d\varrho) * L^1(S^2, d\mu) \hookrightarrow L^2(S^2, d\mu), \tag{A.8}$$

$$L^2(S^2, d\mu) \widetilde{*} L^1(S^2, d\mu) \hookrightarrow L^2(SO(3), d\varrho). \tag{A.9}$$

References

[1] S.T. Ali, J.-P. Antoine, J.-P. Gazeau, U.A. Mueller, Coherent states and their generalizations: A mathematical overview, Rev. Math. Phys. 7 (1995) 1013–1104.

[2] S.T. Ali, J.-P. Antoine, J.-P. Gazeau, Coherent States, Wavelets and Their Generalizations, Springer, New York, 2000.

[3] J.-P. Antoine, P. Carrette, R. Murenzi, B. Piette, Image analysis with two-dimensional continuous wavelet transform, Signal Process 31 (1993) 241–272.

[4] J.-P. Antoine, R. Murenzi, P. Vandergheynst, Two-dimensional directional wavelets in image processing, Internat. J. Imaging Syst. Technol. 7 (1996) 152–165.

[5] J.-P. Antoine, P. Vandergheynst, Wavelets on the n-sphere and other manifolds, J. Math. Phys. 39 (1998) 3987–4008.

[6] J.-P. Antoine, P. Vandergheynst, Wavelets on the 2-sphere: A group-theoretical approach, Appl. Comput. Harmon. Anal. 7 (1999) 262–291.

[7] I. Daubechies, Ten Lectures on Wavelets, SIAM, Philadelphia, 1992.

[8] M. Duval-Destin, M.A. Muschietti, B. Torrésani, Continuous wavelet decompositions, multiresolution, and contrast analysis, SIAM J. Math. Anal. 24 (1993) 739–755.

[9] W. Freeden, U. Windheuser, Combined spherical harmonic and wavelet expansion—A future concept in Earth's gravitational determination, Appl. Comput. Harmon. Anal. 4 (1997) 1–37, and papers quoted therein.

[10] W. Freeden, M. Schreiner, T. Gervens, Constructive Approximation on the Sphere, with Applications to Geomathematics, Clarendon Press, Oxford, 1997.

[11] W. Freeden, Multiscale Modelling of Spaceborne Geodata, Teubner, Stuttgart, 1999.

[12] S.A. Gaal, Linear Analysis and Representation Theory, Springer, Berlin, 1973.

[13] D.M. Healy Jr., D. Rockmore, S.S. Moore, FFTs for the 2-sphere—Improvements and variations, Techn. report PCS-TR96-292, Dartmouth College, Hanover, NH, 1996.

[14] E.H. Lieb, M. Loss, Analysis, Amer. Math. Society, Providence, RI, 1997.

[15] S.G. Mallat, A Wavelet Tour of Signal Processing, 2nd Ed., Academic Press, San Diego, CA, 1999.

[16] M.J. Mohlenkamp, A fast transform for spherical harmonics, PhD thesis, Yale University, New Haven, CT, 1997.

[17] M.J. Mohlenkamp, A fast transform for spherical harmonics, J. Fourier Anal. Appl. 5 (1999) 159–184.

[18] M.A. Muschietti, B. Torrésani, Pyramidal algorithms for Littlewood–Paley decompositions, SIAM J. Math. Anal. 26 (1995) 925–943.

[19] F.J. Narcowich, J.D. Ward, Nonstationary wavelets on the m-sphere for scattered data, Appl. Comput. Harmon. Anal. 3 (1996) 1324–1336.

[20] D. Potts, G. Steidl, M. Tasche, Kernels of spherical harmonics and spherical frames, in: F. Fontanella, K. Jetter, P.-J. Laurent (Eds.), Advanced Topics in Multivariate Approximation, World Scientific, Singapore, 1996, pp. 1–154.

[21] P. Schröder, W. Sweldens, Spherical wavelets: Efficiently representing functions on the sphere, in: Computer Graphics Proc. (SIGGRAPH95), SIGGRAPH, ACM, 1995, pp. 161–175.

[22] E.M. Stein, G. Weiss, Introduction to Fourier Analysis on Euclidean Spaces, Princeton Univ. Press, Princeton, NJ, 1971.

[23] B. Torrésani, Analyse continue par ondelettes, InterÉditions/CNRS Éditions, Paris, 1995, Engl. Transl., SIAM, Philadelphia (to appear).

[24] P. Vandergheynst, Ondelettes directionnelles et ondelettes sur la sphère, Thèse de doctorat, Univ. Cath. Louvain, Louvain-la-Neuve, 1998.

[25] U. Windheuser, Sphärishe Wavelets: Theorie und Anwendung in der physikalischen Geodäsie, PhD thesis, Universität Kaiserslautern, June 1995.